Superalloys 2008
Roger C. Reed, Kenneth A. Green, Pierre Caron, Timothy P. Gabb, Michael G. Fahrmann, Eric S. Huron and Shiela A. Woodard
TMS (The Minerals, Metals & Materials Society), 2008

CREEP-FATIGUE AND THERMO-MECHANICAL FATIGUE OF FRICTION-WELDED IN718/MarM247 DISSIMILAR JOINT.

Masakazu OKAZAKI [1], Motoki SAKAGUCHI [1], Tra Hung TRAN [1], Masaru SEKIHARA [2]
[1] Nagaoka University of Technology, Kamitomioka-Machi 1603-1, Niigata, Japan, 940-2188
[2] Hitachi Ltd., Material Research Laboratory, Saiwai-cho, Hitachi-shi, Ibaraki, Japan, 317-8511

Keywords: Dissimilar metals welded joint, Friction welding, Polycrystalline MarM247-LC, Inconel 718, Creep-Fatigue, Thermo-mechanical fatigue, Heat affected zone, Elastic follow-up, Hydrostatic stress, Failure mechanisms.

Abstract

The high temperature strength of the friction welded superalloy joint between cast polycrystalline Mar-M247 and the forged IN718 alloys has been investigated under low cycle and thermo-mechanical fatigue loadings, in comparison with those of the base materials. The experiments showed that the lives of the dissimilar joints were significantly influenced by the test conditions and loading modes. Not only the lives themselves but also the failure positions and mechanisms were sensitive to the loading mode. Especially under the loading conditions in which the creep-fatigue interaction was pronounced, some specific failure phenomena appeared in the DFW joint. The fracture behavior dependences on the loading modes and test conditions were discussed, based on analyses of the macroscopic elastic follow-up mechanism, the stress state by finite element method, and the inhomogeneous microstructure in the joint.

Introduction

Friction welding is a solid state welding process in which joining can be achieved at a temperature below the melting point [1-6]. It has many advantages: narrow heat affected zone (HAZ) without microfissuring, no filler metals, no special requirement of surface preparation, and no inert atmosphere during welding. Thus, this method is an attractive welding process for the joining of new generation nickel based superalloys. In addition, friction welding also provides the ability to join dissimilar materials, which is difficult to achieve with other types of welding techniques. This is particularly useful for taking full advantage of materials with different upper temperature limits: e.g., a "*blisc*", a composite structure consisting of joined blade and disc alloys. If the hybrid dissimilar superalloy structures are successfully developed, they are expected to make a significant contribution to improve high temperature performance and thermal efficiency of gas turbines. Thus, many efforts have been made to fabricate the advanced hybrid structures [1-7].

During the gas turbine operation period, the hot section components are subjected to many types of damage; e.g., creep, high-cycle fatigue, isothermal low cycle fatigue (LCF) at stress concentration area, thermo-mechanical fatigue (TMF), as well as oxidation and environmental attack [8-12]. Especially in the hybrid or composite structures, thermal stress induced by mismatches in thermal expansion coefficients and thermal conductivities between dissimilar base materials is a critical problem at high temperatures. Thus, TMF failure has been a critical issue here. There is very limited understanding of the TMF and LCF failures for hybrid structures made of superalloys [10].

For monolithic materials, many efforts have been made to understand TMF failure mechanisms and the life criteria for design, reliability and long term durability [8-12]. One traditional method from an engineering point of view is to estimate the TMF failure life from an empirical correlation with the LCF life [9,11]. While this type of approach has been successful for many kinds of polycrystalline alloys, it may not always provide reasonable results for Ni-base superalloys [10]. Superalloys, especially single crystal superalloys, exhibit many fracture behaviors which are not well understood [10-12].

The directions of gas turbine development are not only to achieve high thermal efficiency but also cost reduction for production and maintenance [13]. Thus, repair, recoating and refurbishment technologies for the hot section components are important. Efforts are underway to develop new methods and processes for the repair of hot section components, as well as new solder materials. Friction welding must be successfully applied as a repair technique in the near future. Therefore, basic knowledge on the TMF and LCF of the friction welded parts can provide very useful information to them.

The objective of this work was to investigate the high temperature fatigue strength of a dissimilar friction welded (DFW) joint consisting of cast polycrystalline Mar-M247 and forged Inconel 718 alloys, compared with that of the two base materials; Mar M247-LC and the Inconel 718. Special attention was focused not only on the lives themselves but also on the underlying failure mechanisms.

Experimental Procedures

Fabrication of M247/IN718 Dissimilar Metals Welded Joint.

The welded joint between the cast polycrystalline MarM247-LC and the forged Inconel 718 alloys (hereinafter, denoted by DFW joint) is a main target in this work. The chemical compositions of the base materials; Mar M247-LC and Inconel 718 (hereinafter, denoted by M247 and IN718, respectively) are summarized in Table I. Before the welding, both parent materials had received heat treatments with the following conditions:

solution heat treatment at 1095 ℃ for 1 hour in Ar atmosphere, followed by aging at 720 ℃ for 8 hours in air for IN718; and solution heat treatment at 1232 ℃ for 2 hours in Ar atmosphere, followed by aging at 870 ℃ for 20 hours in air for M247.

The IN718/M247 joints were fabricated by friction welding. Many primary tests were carried out to fabricate an optimal IN718/M247 joint, where the fabrication variables were: rotation speed of base metals, preheating time, compression normal stress to induce frictional heating, duration time of compression stress, upset pressure, upset clearance, upset hold time, and the post weld heat treatment. A final welding condition was determined, based on the following properties of the joint: no significant defects, no significant heat affected zone near the welded interface, and tensile properties comparable to the base materials.

Microstructural characterization near the weld interface was carried out using an electron backscatter diffraction (EBSD) system (JEOL FE-SEM JSM-7000 F) with analytical software (OIM analysis 4.6) as well as optical microscopy. The EBSD patterns were detected by using a charge coupled device camera and image process background subtraction.

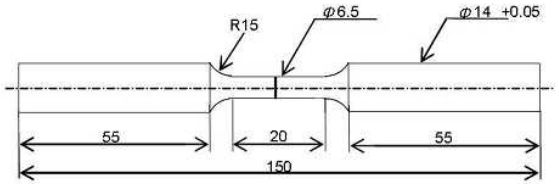

Fig. 1 Geometry of fatigue specimen used.

Mechanical Tests.

From the IN718/M247 joint, solid cylindrical specimens were extracted as illustrated in Fig. 1, where the welded interface was locating at the specimen center, and was oriented normal to the specimen axis. For the purpose of comparison, the specimens of the parent alloys; IN718 and M247, were also prepared.

Using these specimens, low cycle fatigue (LCF) and thermo-mechanical fatigue (TMF) tests were carried out for both the welded joints and their base materials, according to the test conditions summarized in Table II. Here the TMF tests were performed with the mechanical strain cycling superimposed in a synchronized manner on the thermal free expansion strain cycling (see an illustration in Table II). All of the tests were performed under strain-controlled conditions in air by means of a servo-electro-hydraulic test machine so that both material regions equally shared load across the total specimen gauge length. The specimens were heated by a high frequency induction heating system, which provided a uniform temperature distribution along the specimen gauge section within 3 ℃ at 650°C. These temperature distributions were compensated during the natural cooling process in the TMF test. The temperature variation with time was within 3 ℃ during the LCF and TMF tests. Here, the test temperature during the TMF and LCF tests was represented and controlled through R type of thermocouples welded near the shoulder. This method did not encourage cracking from the welded part of thermocouples, an undesirable phenomenon often

Table I Chemical composition of base metals. (wt.%)

Composition	Ni	Cr	Co	Mo	W	Ta	Nb	Al	Ti	Fe	Mn	Si	C	B	Zr	Hf
IN 718	52.5	19	-	3	-	-	5.1	0.5	0.9	18.5	0.2	0.2	0.04	-	-	-
M247	60	8.3	10	0.7	10	3	-	5.5	1	-	-	-	0.14	0.015	0.05	1.5

Table II Summary of LCF and TMF test conditions.

Specimen	Test type	Strain wave form	Temp. [C]	Strain ratio	Strain rate [1/sec]	Tension hold time	Remarks
DFW joint	LCF	fast-fast	650	-1	5×10^{-4}	0	f-f LCF
		slow-slow			10^{-5}	0	s-s LCF
		tension hold			10^{-5}	10 min	tension hold LCF
	TMF	out-of-phase	300-650	-1	10^{-4}	0	OP TMF
		in-phase			10^{-5}	0	IP TMF
M247	LCF	fast-fast	650	-1	10^{-5}	0	f-f LCF
		tension hold			10^{-3}	10 min	tension hold LCF
IN718	LCF	fast-fast	650	-1	10^{-3}	0	f-f LCF
		slow-slow			1.7×10^{-5}	0	s-s LCF
		tension hold			10^{-4}	10 min	tension hold LCF

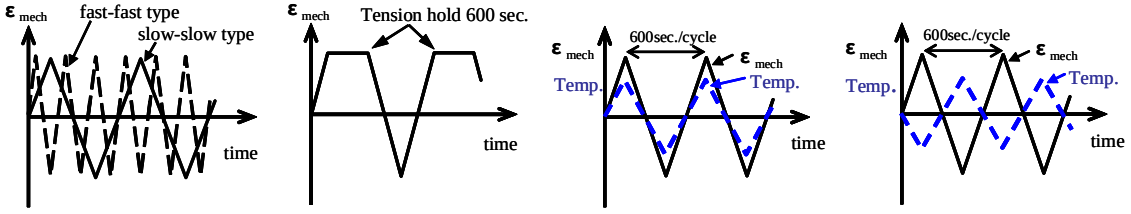

(a) Low cycle fatigue (b) Tension hold LCF (c) IP TMF (d) OP TMF

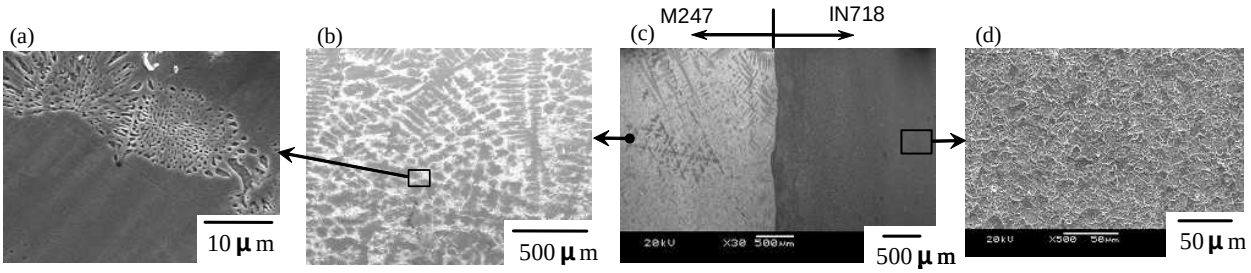

Fig. 2 Microstructure of the DFW joint. (a)Partially eutectic structure in M247, (b)dendritic structure of M247, (c)overview of IN718/M247 interface and (d)fine grains of IN718.

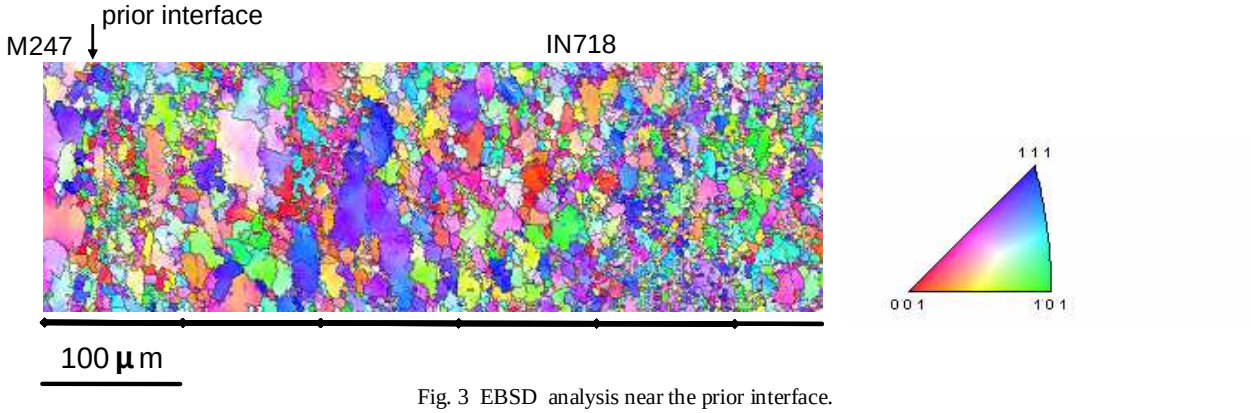

Fig. 3 EBSD analysis near the prior interface.

experienced in fatigue tests of superalloys.

In the isothermal LCF tests, the primary experimental strain variables were strain range and strain rate, denoted by the "f-f" and "s-s" tests in Table II, in which the repeated strain rates were high and low enough so that creep was insignificant and significant, respectively. Other variables included test temperature, strain ratio, and hold time introduced at the maximum tensile strain. Here, the LCF test with a hold time will be denoted by "tension hold test". In the TMF test, the experimental variables were strain range and temperature/strain phase angle: 0 degree (in-phase condition) and 180 degree (out-of-phase condition), respectively.

The number of cycles to failure in the TMF and LCF tests was defined by the number of strain cycles at which the tensile stress was reduced by 50 % from the stable value. Special attention was paid not only to the failure lives of the IN718/M247 DFW joint in comparison with those of the base materials, but to the failure modes and mechanisms which depended on both the loading modes and the test conditions. After the mechanical testing, the morphology of fracture surfaces was observed by scanning electron microscopy (SEM); JEOL 6360 coupled with energy dispersive spectroscopy (EDS). Metallographic sectioning perpendicular to the crack plane was also performed to confirm the crack initiation site.

Results

Metallographs of IN718/M247 DFW Joint

Hereinafter, all the experimental results will be shown for the DFW specimens to which the post weld heat treatment (PWHT) was given of 720 ℃ for 2 hours in air. The microstructure near the welded interface is shown in Fig. 2. The M247 and the IN718 far from the welded interface had conventional microstructures. The M247 possesses dendritic structure which consists of very large polycrystalline grains of millimeter order in diameter (Fig.2(b)). On a microscopic level, the M247 revealed a γ/γ' composite structure containing partially eutectic structure at the dendritic boundaries (see Fig. 2(a)), where the volume fraction of γ' phase is about 0.5 μm in diameter and 55 % in volume fraction. On the other hand, the IN718 away from the weld interface was composed of very fine grains of about 10 μm diameter (see Fig. 2(d)).

Near the welded interface, there were no visible defects along the welded line. On a microscopic scale, the joint reveals a very complicated morphology and characteristics, as indicated by the EBSD analysis shown in Fig. 3. The grain size distribution on the IN718 side is given in Fig. 4. It is found from Figs. 3 and 4 that the grain size distribution fluctuated: very fine just near the prior interface, significantly coarsened with large scatter at 200-300 μm from the interface, then back to the original state. However, the EBSD analysis shows that insignificant texture has not developed through the whole area.

Figure 5 depicts the hardness distributions near the interface of the joint just after the PWHT. While the hardness on the IN718 side is nearly comparable on average to that on the M247, there is more scatter in the latter. This can be attributed to randomly oriented large grains in this material (Fig. 2). A heat affected zone with lower hardness seems to be formed at several hundreds microns from the prior interface on IN718 side (Fig. 5). However, as shown in Fig. 3, texture has not significantly developed there. It has been confirmed by other researchers that a heat affected zone

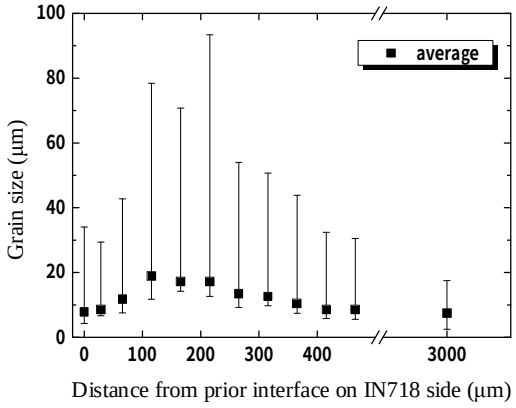

Fig. 4 Grain size distribution on IN718 side near the prior interface.

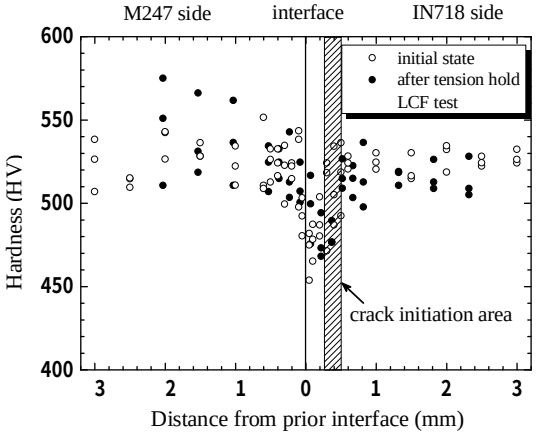

Fig. 5 Hardness distribution near the interface.

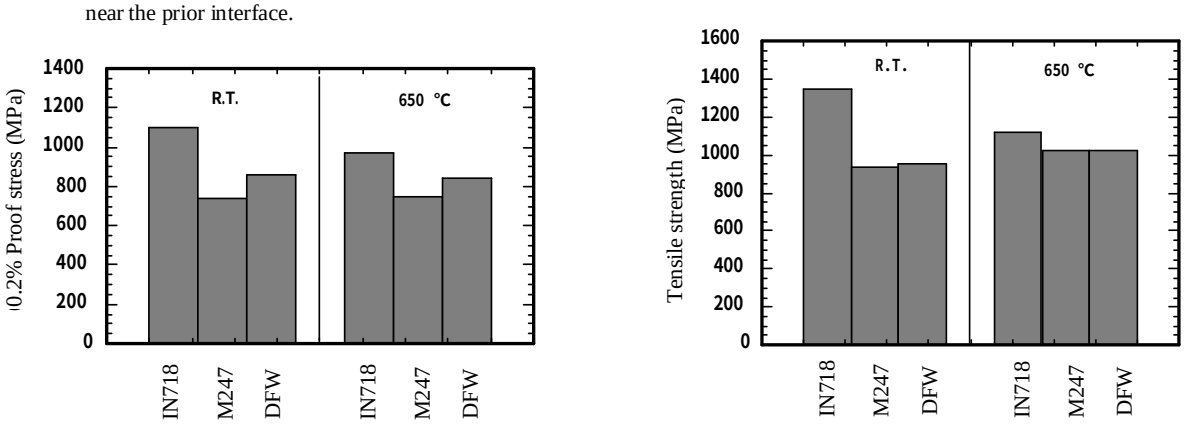

Fig. 6 Summary of tensile tests at (a) Room Temperature, and (b) at 650℃.

(HAZ) was often formed associating with significant hardness drop (i.e., soft HAZ) when the IN718 was welded [2, 3]. Whereas the formation of soft zone was strongly dependent on the PWTH conditions [3], dissolution of the main strengthening precipitates, γ' $Ni_3(Al,Ti)$ with a $L1_2$ structure and γ"($Ni_3(Nb)$ with a DO_{22} structure, might occur during the welding process [3], and be responsible for the soft HAZ in this work.

Tensile Test of DFW Joint.

The result of tensile tests of the parent materials and that of the DFW joint are summarized in Fig. 6. The proof stress and the tensile strength of IN718 are higher than those of M247 at room temperature and 650 ℃. The DFW joint reveals intermediate properties between the two base materials. The final rupture of the joint took place on the Mar M247 side, apart from the prior interface. This is not surprising, comparing the relative strength of the base materials at this test temperatures.

TMF and LCF Failures.

The LCF and TMF lives of the DFW joint are summarized and compared with those of the parent materials in Figs.7 through 9. Note that the vertical axis of these figures for the TMF test denotes mechanical strain range, $\Delta\varepsilon_{mech}$, in which the apparent thermal free expansion strain is excluded. $\Delta\varepsilon_{mech}$ corresponds to strain range itself for the LCF tests. On the basis of $\Delta\varepsilon_{mech}$, it is possible to directly compare the TMF lives with the LCF ones. It is clear from these figures that the lives of the DFW joints are significantly influenced by the test conditions and the loading modes. The details of the fatigue lives and the fracture behaviors will now be considered.

It is clear from Fig. 7 that the LCF life of IN718 parent material is longer than that of M247 under a fatigue dominant condition or under the f-f cycling. Under the same strain rate condition, the DFW joint possesses the intermediate LCF life between the two base materials. Reflecting this relative order in fatigue strength, the DFW failed on the M247 side away from the weld interface, see illustration summarized in Fig.10. SEM observation indicated that the fatigue crack was nucleated from inter-dendritic boundaries of eutectic pools, with similar morphologies to those given in Fig. 12.

When the strain rates were decreased, the LCF life of the IN718 decreased (Fig.7). The LCF life of DFW, as well as that of the IN718 base material, also decreased with decreasing strain rate. It is important to note that the final failure of the DFW took place on the IN718 side very near the welded interface, a different

failure position from that under the fatigue dominant condition (Fig.10).

The LCF lives of the DFW joint and the base metals for tests with a tension hold time of 10 min. at maximum tension strain are shown in Fig. 8, compared with those under the f-f and s-s LCF lives of DFW joint. The tension hold significantly reduced the fatigue lives, compared with the f-f LCF and the s-s LCF. While the reduction is seen not only in the base materials but in the DFW as well, it is more significant in the latter. In addition, the lives of the joint are significantly shorter than those of both parent materials. Failure at a high strain range of $\Delta\varepsilon_{mech}$=1.0% was associated with the specimen buckling on the M247 side (see Fig.8). This was not an experimental mistake, but seemed reasonable, as will be discussed in the next section.

The fracture morphologies of the DFW specimen under the tension hold test are given in Fig. 11. It is found that the fracture was led by cracks that propagated in the narrow HAZ area on the IN 718 side about 300 μm from the prior interface (Fig.11(c)), associating with significant intergranular fracture (Figs. 11(a) and (b)). Although the IN718 had longer failure life than the M247 (see Fig. 8), the failure of the DFW joint originated from the IN718 side. This behavior is more or less similar to the creep-fatigue failure in the steel welds, a so-called *Type IV cracking*, where the damage has been concentrated at the narrow HAZ area with low hardness [7]. This will be discussed again in the next section. Summarizing these observations, a different failure mode occurred in the DFW joint when creep-dominant loadings were applied to the DFW.

The in-phase (IP) and out-of-phase (OP) TMF lives of the DFW joints are compared with the LCF lives in Fig. 9, which shows that the temperature/strain phase angles did not significantly affect the TMF lives. It is also found from Fig. 9 that the TMF lives of the joints were almost comparable to the LCF lives under s-s cycling in this work. Under these conditions, all the DFW specimens failed on the M247 side away from the welded interface. The fracture behavior was also very similar to that under the fatigue dominant loading condition (i.e., f-f LCF test), where the crack often originated from the eutectic at dendritic boundaries (see Fig. 12). Thus, a semi-empirical rule can be applied, that the TMF lives of the DFW joint under IP and OP conditions can be approximately estimated from the LCF lives measured at the maximum and at the intermediate temperatures of the TMF tests, [9,11].

Discussions

As shown in the previous section, some specific failure phenomena not estimated from the tests of monolithic materials appeared in the DFW joint under the tension hold creep-fatigue loading condition. Accordingly, some mechanistic and metallurgical considerations of these specific fracture behaviors is necessary. It is important to note that the life of the DFW joint was significantly reduced in comparison with those of the two base materials, and the damage evolved in the narrow HAZ area was associated with the intergranular fracture mode.

In steel weldments, failure relating to the HAZ have also been often observed. This failure is called *Type IV cracking* [6,7], where the lower hardness HAZ produced by complex thermal histories during the welding process is the preferential failure site

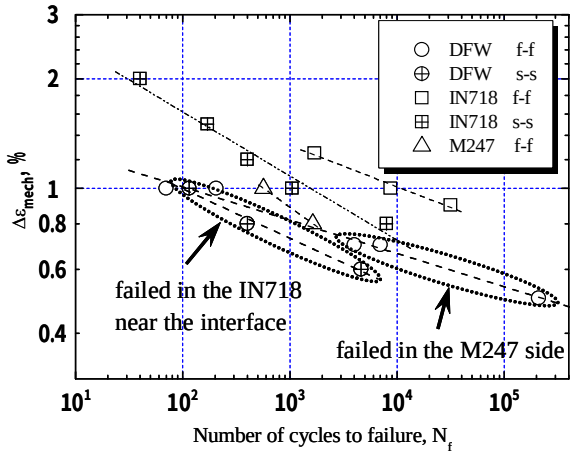

Fig. 7 Summary of LCF lives of the DFW joint, compared with those of the parent materials.

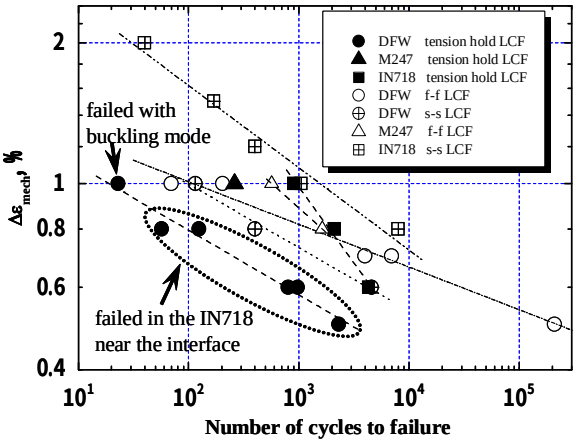

Fig. 8 Tension hold LCF lives of the DFW joint compared with those under other test conditions, and with those of the parent materials.

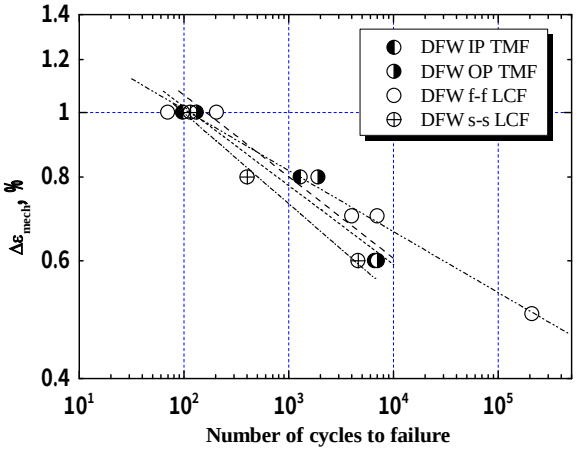

Fig. 9 Comparison of TMF lives of the DFW joint compared with those of the parent materials.

for creep. Referring to Figs. 2 through 5 and 8, some similarities are seen between the Type IV cracking and the present DFW failure. It is evident that the mechanical properties of the HAZ could be poor and therefore responsible for the preferential failure there. However, the underlying failure mechanism is apparently more complex than expected. Note that the failure has taken place on the M247 side under the fatigue dominant condition as well as in the monotonic tensile test (see Figs. 6 and 7). In the other words, why did the DFW not fail at the "*weaker*" HAZ under these conditions?

Comparing creep resistance of IN 718 with that of M247, the latter could be appreciably higher than the former at the present test temperature range [14, 15]. In this work, cyclic loading is repeated under strain-controlled conditions for DFW specimens consisting of the two materials. Figure 13 schematically depicts a possible deformation mechanism of the DFW joint under creep-fatigue loading with tension hold time, where for simplicity the IN718 and the M247 are assumed to be visco-elastic and elastic materials, respectively. The right- and left-hand side horizontal axes express the average strain range shared in the IN718 and M247 sides, respectively. The vertical axis is the external load applied to the specimen. Consider a case in which the DFW joint is subjected to the strain-controlled LCF loading with tension hold time. When the strain cycling starts from zero to maximum tensile strain, the shared strains follow from the origin, O, to the points *a* on the M247, and to *A* on the IN718, respectively. When the tension hold period starts, stress relaxation will occur under a fixed strain. Since the creep deformation resistance of the IN 718 could be lower, the states change from the points A to B for the IN 718, and *a* to *b* for the M247, associating with the stress relaxation, $\Delta\sigma_r$. During this hold time, the stress in the M247 will be relaxed only elastically. Through this mechanism the total strain of the DFW joint is kept constant during the strain hold time. However, this type of relaxation may lead to eccentric creep deformation only on IN718 side. When the loading is reversed, the stress is unloaded and relaxed elastically in both materials (B to C, and *b* to *c* in Fig.13). For the next strain cycle (A' to B' in Fig.13), a tensile creep strain is again accumulated on the IN718 side. Thus the progressive creep deformation with ratchetting may evolve only in the IN718. This mechanism will be called the elastic follow-up mechanism in this work.

This phenomenon may lead to a change of the loading ratio with strain cycling in the creep-fatigue tests. Under the creep-fatigue loading with tension hold time, the change must be toward compressive direction. Figure 14 shows the change of stress ratio with the number of cycles during the tension hold LCF test of the DFW specimen. It is found from Fig.14 that the stress ratio of the DFW joint continued to decrease with cycles monotonically in the compressive direction, supporting the elastic follow-up mechanism described. When the elastic following-up phenomenon is very pronounced, it may induce a specific failure mode of the DFW joint. In fact, the DFW specimens failed with buckling under high strain range (see Fig. 8). This also agrees with the estimation from Fig. 14. These matters support that the elastic follow-up mechanism may be one of the major reasons for the specific failure behaviors of the DFW joint under creep-fatigue loading condition.

The elastic follow-up mechanism itself is too macroscopic to give a reasonable explanation to the localized damage

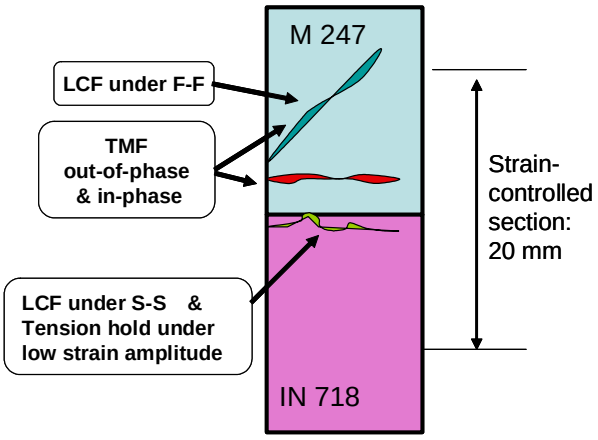

Fig. 10 Schematic illustration showing the failure sites depending on the loading conditions and modes.

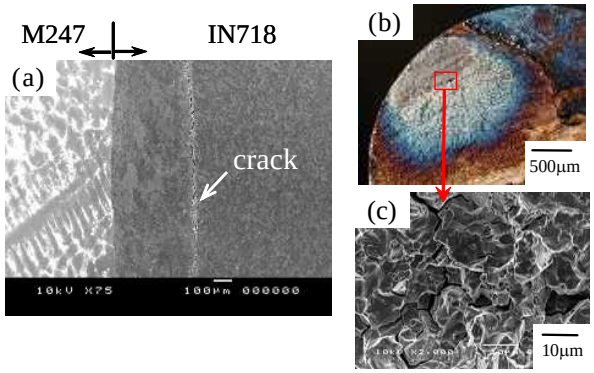

Fig. 11 Fracture behavior of the DFW joint under the tension hold LCF test, showing (a) Overview of fracture surface, (b)Intergranular fracture surface, (c) predominant cracking at the HAZ.

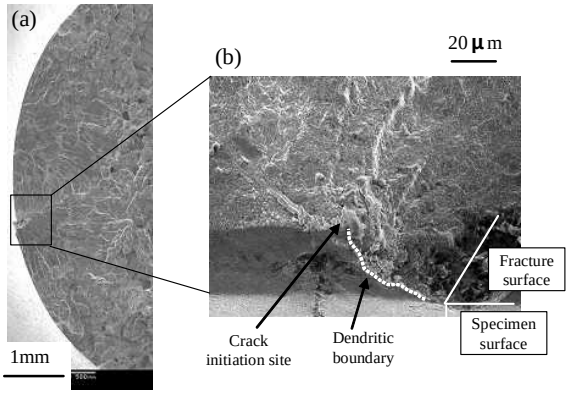

Fig. 12 TMF failure originated from the M247 side under the TMF test. (a) Overview of fracture surface, (b) Cracking from the dendritic boundaries.

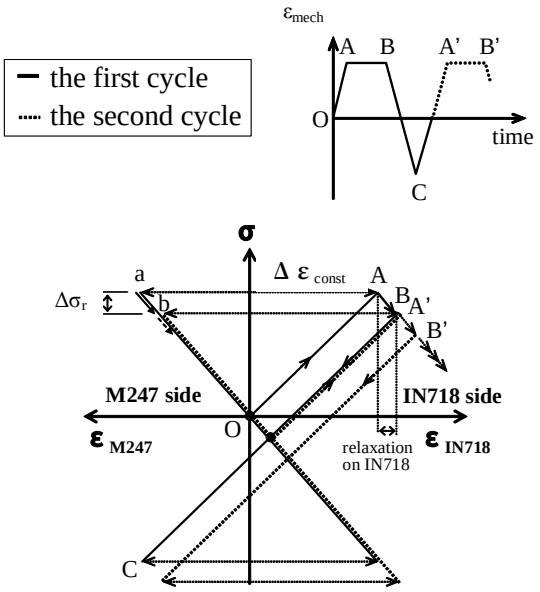

Fig. 13 Elastic follow-up mechanism possible in the DFW joint under tension hold test.

Table III Mechanical properties used for FEM calculation.

	Young's modulus, GPa	Poisson's ratio
IN718	176.3	0.28, 0.4, 0.5
M247	183.3	0.3

evolution at the HAZ on the IN 718 side. In order to expand discussions to a more local level, finite element method (FEM) analysis was carried out to estimate the stress state near the weld interface. The calculation was conducted in an elastic state, assuming plane strain condition. The software employed is ANSYS 6.3, where the numbers of elements and nodes were about 16726 and 24634, respectively. The mechanical properties used for the calculation are summarized in Table III. A visco-elastic-plastic analysis is more preferable for quantitative discussions. However, an elastic analysis is adequate for the present purpose, as the levels of viscosity and plasticity in the narrow HAZ has not been clear.

The distribution of the hydrostatic stress component, $\sigma_H=(\sigma_1+\sigma_2+\sigma_3)/3$ (where σ_1, σ_2 and σ_3 are principle stresses), is illustrated in Fig. 15 as a function of the Poisson ratio of IN718 material. The increase in Poisson ratio from 0.28 to 0.5, qualitatively corresponds to a development of plastic deformation. It is found from Fig. 15 that the σ_H peaks near the prior interface on the IN 718 side, and the peak value increases with the progress of plastic deformation in IN718. The peak area of σ_H approximately corresponds with the area where the creep-fatigue cracks were preferentially initiated and propagated in the DFW joint, associated with intergranular fracture (see Fig. 11(c)). Since σ_H is a mechanical factor to promote creep cavitation, it can be concluded that the creep-fatigue failure was localized at the HAZ area due to the increase of σ_H there.

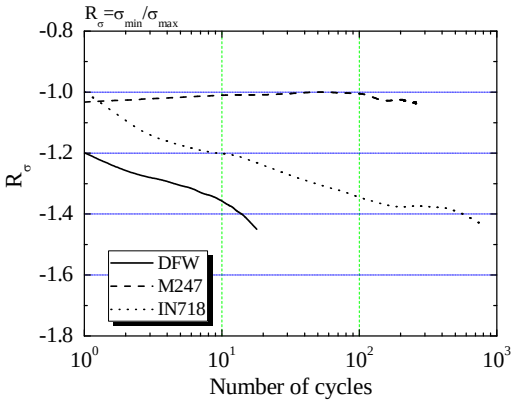

Fig. 14 Change of stress ratio with the number of strain cycles in DFW joint under tension hold test.

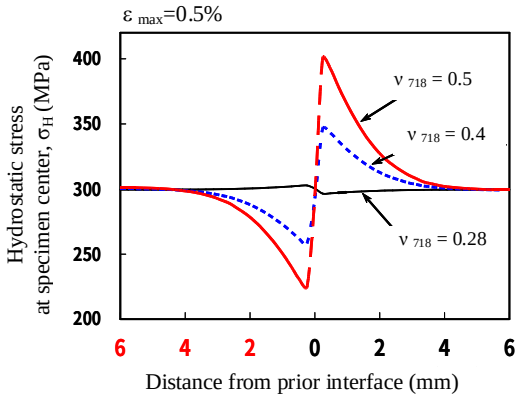

Fig. 15 Distribution of hydrostatic stress component calculated by the FEM analysis.

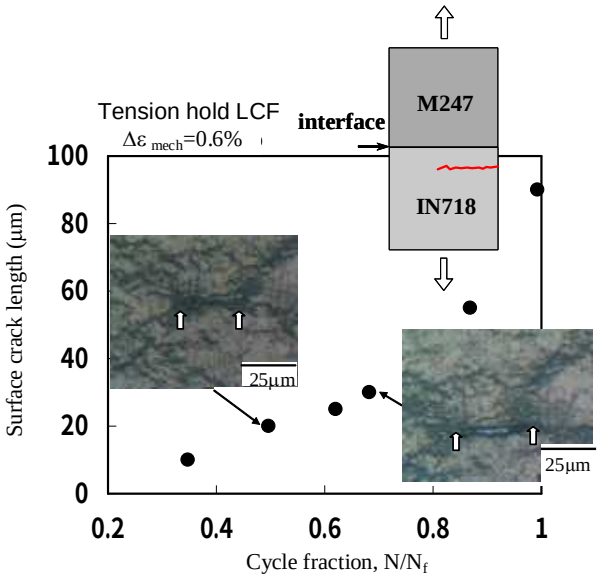

Fig. 16 Small crack initiation and the subsequent propagation behavior in DFW joint under tension hold test.

In order to confirm this situation, tension hold LCF tests were also carried out to observe crack initiation and the subsequent propagation behavior. Figure 16 expresses the small crack propagation behavior with number of strain cycles. Note that the results were determined using a smooth DFW specimen, by employing a replication technique with acetyl cellulose film. The small crack began to initiate at 20 % cyclic life fraction and then continuously grew from 20μm to 200μm in length at the HAZ area normal to the loading axis, with coalescence of other small cracks.

In addition, it is important to point of a possible contribution of environmental effect to the specific failure under the tension hold LCF test, such as stress assisted grain boundary oxidation (SAGBO), because the present experiments were conducted in air. It has been confirmed that there was deleterious effect of oxygen on the high temperature strength of IN718, especially under creep loading [16, 17]. However, further investigation is needed to make clear this point.

Summarizing these discussions, the following factors are contributing to the specific creep-fatigue failure at the narrow HAZ in the DFW joint: the inhomogeneous microstructure, lower hardness, and the promoted hydrostatic stress component associated with an elastic follow-up mechanism.

Summary

In this work, a DFW joint between cast polycrystalline Mar-M247 and forged Inconel 718 alloys (IN718/M247 DFW joint) has been fabricated by friction welding. The high temperature low cycle fatigue life and thermo-mechanical fatigue of the joint were quantified and compared with those of the base metals. It was shown the lives as well as the failure positions of the DFW joint were significantly influenced by the test conditions and loading modes. Especially under creep-fatigue loading conditions, a unique failure phenomena appeared in the DFW joint. Here, the life was significantly reduced compared with those of the base materials, and the damage evolved at the narrow HAZ area in a concentrated manner with intergranular fracture. It was shown that both the elastic follow-up mechanism and the promoted hydrostatic stress component, as well as the inhomogeneous microstructure, were important factors contributing to these failures.

Acknowledgements

Financial support by Grant-in-aid from the Ministry of Education, Japan (No. 19860036) is greatly acknowledged.

References

[1] F. Daus, H.Y. Li, G. Baxter, S. Bray, P. Bowen, "Mechanical and microstructural assessments of RR1000 to IN718 inertia welds - effects of welding parameters", Mater. Sci. Tech., Vol.23, No.12, (2007), pp.1424-1432.

[2] Z.U. Huang, H.Y. Li, M. Preuss, M. Karadge, P. Bowen, S. Bray, G. Baxter, "Inertia friction welding dissimilar Nickel-based superalloys alloy 720Li to IN718", Metall. Mater. Trans., Vol.38A, pp.1608-1619, (2007)

[3] P. Adam, "Welding of high strength gas turbine alloys", Applied Science Publisher Ltd, (1978), pp.737-768.

[4] C.T. Sims, W.C. Hagel, The Superalloys 72, John Wiley, New York, (1972), pp.509-532.

[5] M. Preuss, P.J. Withers, G.J. Baxter, "A comparison of inertia friction welds in three nickel base superalloys", Mater. Sci. Eng., Vol. A437, (2006), pp.38-45.

[6] M. Okazaki, Y. Mutoh, T. Yada, M. Yamaguchi,"Creep-Fatigue Fracture behavior of dissimilar metal electron beam welded joint ", J. Soc. Mater. Sci., Japan, Vol.36, (1987), pp.1239-1245.

[7] T.H. Hyde, A.A. Becker,"Creep crack growth in welds: A damage mechanics approach to predicting initiation and growth of circumferential cracks", Int. J. Press. Vess. & Piping, Vol.78, (2001), pp.765-771.

[8] R.V.Miner, "Fatigue", Superalloys II, ed. C.T. Sims, W.C.Hagel, Wiley, New York, (1987) pp.263-287

[9] S. Taira, M. Fujino, R. Ohtani,"Collaborative study on thermal fatigue properties of high temperature alloys in Japan", Fatigue Eng. Mater. Struc., Vol.1, (1979), pp.495-500.

[10] M. Okazaki, Y.Yamazaki and K.Take, "Themo-Mechanical and Isothermal Low-Cycle Fatigue Strengths of Ni-Base Superalloys and the Protective Coatings at Elevated Temperatures",ASTM, STP 1428, Thermo-Mechanical Fatigue Behavior of Materials", 180-196,(2003).

[11] M. Sakaguchi, M. Okazaki, "Thermo-mechanical and low cycle fatigues of single crystal Ni-base superalloys; Importance of microstructure for life prediction", JSME international, Vol.49A, No,3, (2006), pp.345-354.

[12] M.Sakaguchi, M.Okazaki, "Fatigue life evaluation of a single crystal Ni-base superalloy, accompanying with change of microstructural morphology", Int. J. Fatigue, Vol.29, No.9, (2007), pp.1959-1965.

[13] M. Okazaki , I. Ohtera and Y. Harada, "Damage Repair in CMSX-4 Alloy without Fatigue Life Reduction PenaltyV, Metall. Trans.-A, vol.35-A, pp. 535-543, (2004).

[14] C.R. Brinkman, M.K. Booker,"Creep and creep-rupture behavior of alloy 718", J.L. Ding, Superalloys 718, 625 and Various Derivatives, TMS, (1991), pp.519-536.

[15] M.V. Nathal, R.D. Maier and L.J. Ebert,"Influence of cobalt on the tensile and stress-rupture properties of the nickel-base superalloy MAR-M247", Metal. Trans. A, Vol.13A, (1982), pp. 1767-1774.

[16] R. Molins, G. Hochstetter and E. Addrieu, "Oxidation effect on the fatigue crack growth behavior of alloy 718 at high temperature", Acta Mater., Vol.45, (1997), pp.663-674.

[17] J.A. Pfaendtner and C.J. McMahon Jr., "Oxigen-induced intergranular cracking of Ni-base alloy at elevated temperatures – An example of dynamic embrittlement", Acta Mater., Vol.49, (2001), pp.3369-3377.